agriculture

MDPI

Article

Strategies for Selecting Potentially Effective Biofumigant Species for Optimal Biofumigation Outcomes

Juan Manuel Arroyo, Jose Soler, Rubén Linares and Daniel Palmero *

Departamento de Producción Agraria, Escuela Técnica Superior de Ingeniería Agronómica, Alimentaria y de Biosistemas, Universidad Politécnica de Madrid, Avenida Puerta de Hierro, 4, 28040 Madrid, Spain
* Correspondence: daniel.palmero@upm.es

Abstract: Soil-borne diseases threaten sustainable agriculture, traditionally managed by chemical fumigants, whose use is now restricted due to environmental and health concerns. This study evaluates the biofumigation potential of *Brassicaceae* species, specifically *Brassica carinata* A. Braun., *Brassica juncea* (L.) Vassiliĭ Matveievitch Czernajew., *Raphanus sativus* L., and *Sinapis alba* L., cultivated in central Spain. Field trials across two growing cycles assessed biomass production, glucosinolate (GSL) concentration, photosynthetically active radiation (PAR) interception, and radiation use efficiency (RUE). Biomass production varied across species and sampling dates, with *S. alba* and *R. sativus* outperforming other species in shorter cycles, while *B. juncea* and *B. carinata* showed a more efficient GSL profile regarding soil-borne disease control, particularly in aliphatic GSLs like sinigrin. Results highlight *B. juncea* and *B. carinata* as potent biofumigants due to their high GSL levels, whereas *S. alba* and *R. sativus* are more suited to early biomass production. The study also explores the chlorophyll content index (SPAD) as a potential field indicator of GSL concentration, providing a practical approach for optimizing biofumigation timing. These findings support the selection of specific *Brassicaceae* species adapted to climatic conditions and crop cycles for effective biofumigation in sustainable agricultural practices.

Keywords: sustainable agriculture; glucosinolates (GSL); *Brassicaceae* species; soil-borne diseases

Academic Editors: Aocheng Cao and Dongdong Yan

Received: 1 November 2024
Revised: 1 January 2025
Accepted: 9 January 2025
Published: 11 January 2025

Citation: Arroyo, J.M.; Soler, J.; Linares, R.; Palmero, D. Strategies for Selecting Potentially Effective Biofumigant Species for Optimal Biofumigation Outcomes. *Agriculture* **2025**, *15*, 147. https://doi.org/10.3390/agriculture15020147

1. Introduction

Soil-borne diseases pose a significant threat to sustainable agricultural production, primarily impacting crop yields and quality through infections caused by fungi, bacteria, and nematodes. Traditional control measures often rely on chemical fumigants. However, the negative environmental effects, health hazards, societal concerns, and the development of new environmental strategies, such as the "Farm to Fork Strategy", have heavily restricted the use of these synthetic chemical compounds. This growing concern has spurred the search for sustainable alternatives that may reduce the quantity and toxicity of synthetic chemicals applied to agricultural fields, with biofumigation emerging as a particularly promising strategy [1–3].

Although some cover crops have the potential to suppress soil-borne pests and soil-borne diseases via several mechanisms, including being a non/poor host, which reduces pest and disease abundance by starvation, or trap crops that host pests but prevent pest reproduction [4], one of the most effective mechanisms is biofumigation.

The term biofumigation was initially proposed by Kirkegaard et al. [5]. Although initially defined as the cultivation of specific plants that naturally produce bioactive compounds with biocidal properties, followed by the incorporation of plant residues into the

soil through chopping and rapid mixing [3,6,7], biofumigation now encompasses various application methods. These include cover cropping, whole plant incorporation, and the use of isolated plant products, such as industrially formulated defatted seed meals or concentrated applications of plant essential oils or distilled essences [2,8,9].

While various species and residues have been investigated for biofumigation (e.g., *Allium* spp., *Lavandula* spp., *Sorghum* spp., *Tagetes lucida* Cav, *Azadirachta indica* A.Juss) [9–16], studies have shown that plants of the *Brassicaceae* family are among the most effective. These plants grow rapidly and produce large amounts of biomass [17,18], and some species synthesize high levels of glucosinolates (GSLs) in their tissues.

Due to their high GSL concentrations, species of the genera such as *Brassica*, *Raphanus*, *Sinapis*, and *Eruca* are the most commonly used for biofumigation [16,19–21]. Glucosinolates are secondary metabolites found in some plants (e.g., the *Brassicaceae*, *Capparidaceae*, *Tropaeolaceae*, *Moringaceae*, and *Amaryllidaceae* families) [7,22]. They are composed of β-thioglucoside N-hydroxysulfates (a common functional group), with a side group (R—a variable aglycone side chain derived from one of eight natural amino acids) and a sulfur-linked β-d-glucopyranose moiety [23]. The R group is retained in the resulting isothiocyanates (ITCs), influencing their biocidal activity [24,25].

The decomposition of *brassica* tissues and the enzymatic hydrolysis of GSLs by myrosinase produce toxic ITCs, in addition to other compounds such as thiocyanate, nitriles, organic cyanides, methyl sulfide, dimethyl sulfide, and methanethiol, formed through various chemical reactions. Although these additional compounds are typically less toxic than isothiocyanates, they are often present in large quantities and may also contribute to biofumigation [26–28]. Among these compounds, notably, ITCs are highly effective for disease control due to their broad-spectrum antimicrobial properties [20,26,28,29].

In general, the highest GSL concentrations are found in seeds, followed by aboveground and below-ground tissues [19,30,31]. Glucosinolate concentration in seeds is typically 8–10 times higher than in other parts of the plant [8], although it varies with growth stage, environment, and species interactions [30,31].

High ITC levels are needed for effective soil disinfection through biofumigation. For example, soil sterilization is calculated at effective values of 517 to 1294 μmol/g soil of methyl isothiocyanate [32]. However, lower ITC concentrations in the soil (<1 μmol/g soil of benzyl, 150 μmol/g soil of allyl or 182 μmol/g soil of methyl isothiocyanate) are sufficient to control most pests and soil-borne diseases, such as *Folsomia fimetaria*, *Verticillium dahliae*, or larvae of the *Otiorhynchus sulcatus* (F.) [33–35]. It is important to note that while biofumigation aims to achieve disease control, it does so by using targeted doses of glucosinolates, which release ITCs without the need for complete soil sterilization. This aligns with the goal of preserving soil biodiversity and the ecosystem services it mediates, in line with EU policies that promote sustainable agricultural practices. Thus, although plant GSL concentration is crucial to the success of biofumigation, the key factor is the controlled release of ITCs into the soil, allowing for effective disease suppression while maintaining ecological balance [36].

Biofumigation has several potential benefits, not only providing a natural alternative to synthetic fumigants with reduced environmental and human health risks but also offering a diverse array of bioactive chemicals that soil-borne diseases may not be adapted to resist. Biofumigation contributes organic matter to the soil, improving soil structure, enhancing soil health through erosion prevention, increasing nutrient availability, reducing nitrogen leaching, stimulating beneficial or pathogen-suppressive microbial communities, and suppressing weed pressure, potentially reducing costs for growers) [2,16,24].

Several studies have shown the effectiveness of biofumigation is linked to GSL tissues concentration but also, especially, when it is linked with each species' capacity for biomass

accumulation [37,38]. In turn, biomass accumulation ability is influenced by species' ability to intercept and utilize photosynthetically active radiation (PAR), as well as their RUE [18].

Several studies have shown that *R. sativus* and *S. alba*'s biomass accumulations are greater than those of other cover crops [17,18]. These species can achieve 115.8 g/m^2 and 138.2 g/m^2 of dry matter biomass, respectively, in summer–autumn cycles under water-limited conditions in central Bohemia [18] and 480 g/m^2, and 452 g/m^2 of dry matter biomass, respectively, in summer–autumn cycles under Northern European conditions (The Netherlands and Germany) [18]. These results demonstrate the high adaptability and growth potential of these species.

In general, this behavior is due to the high PAR interception of these species (between 520 and 559 MJ/m^2 under Northern European conditions) rather than to high RUE [17,18,39].

Although Arnault et al. [15] showed that crucifers' RUEs (*R. sativus*, 0.8 g/MJ or *S. alba*, 0.85 g/MJ) were lower than those of other cover crops, such as *Avena strigosa* Schreb. (1.18 g/MJ), under optimal conditions (nitrogen application and planting density) *B. napus* can show high RUE (1.33 g/MJ) [39].

This study aims to evaluate the potential of biofumigant species for use in extensive horticultural crops in central Spain. Specifically, the research focuses on identifying species that not only possess high levels of bioactive GSLs but also demonstrate effective adaptation to the region's climatic conditions and cultivation cycles. By evaluating these species in terms of biomass production, GSL concentration, and seasonal variations, this study seeks to optimize biofumigation practices that can be integrated into local crop rotation and management systems.

2. Materials and Methods

2.1. Location and Soil and Climatic Conditions

The trial was conducted at the Experimental Fields of ETSIAAB (Polytechnical University of Madrid) during the 2022–2023 and 2023–2024 agricultural growing cycles, hereafter referred to as first and second cycle, respectively. The soil in the experimental plot has a sandy loam texture, with a basic pH of 7.8 and low organic matter content (1.2%). The carbon/nitrogen (C/N) ratio is 8, and the electrical conductivity (EC) measured in a 1:5 extract is 0.16 dS/m. High levels of calcium (Ca $\geq$ 2500 mg/kg), magnesium (Mg $\geq$ 250 mg/kg), potassium (K $\geq$ 300 mg/kg), and phosphorus (P $\geq$ 60 mg/kg) were detected, based on analyses carried out on four soil samples, one per trial block, collected from the 0–30 cm and 30–60 cm horizons.

According to the Köppen classification, the climate in the region is temperate with dry or hot summers (Csa), with a mean annual rainfall of 379 mm and a mean annual temperature of 14.6 °C (Castilla-La Mancha, i.e., Toledo, Ciudad Real, Albacete). According to the UNESCO-FAO classification, the specific climate at the trial site (Madrid) is described as a "temperate climate with mild winters, xeric, attenuated thermomediterranean", with an average annual rainfall of 421 mm and an average annual temperature of 15.1 °C.

The weather conditions in 2022 and 2023 in terms of thermal and rainfall patterns were very different: 2022 had a very dry autumn and cold winter with a prolonged frost period, whereas 2023 was characterized by abundant rainfall in autumn and a mild winter (Figure 1).

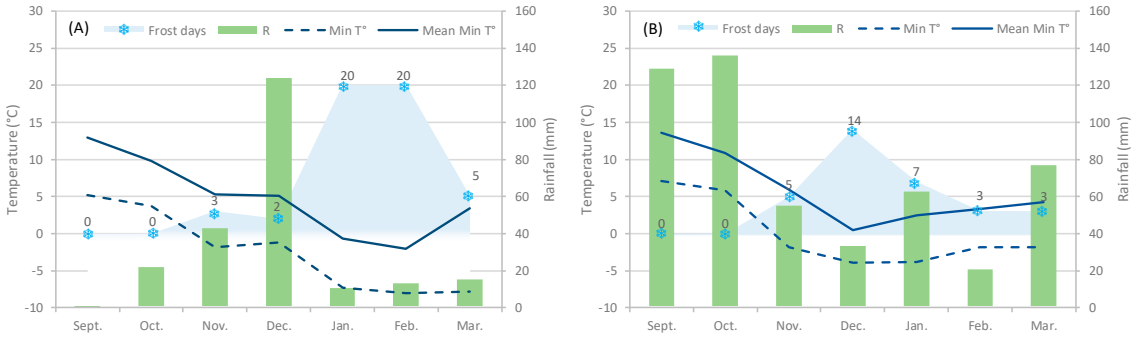

Figure 1. Weather data during 2022–2023 (**A**) and 2023–2024 (**B**) growing seasons. Frost days: days per month when the minimum temperature was below 0 °C; R: rainfall; Min T°: minimum temperature; and Mean Min T°: mean minimum temperature.

2.2. Experimental Design

The experimental design followed a randomized block layout with four replicates, with the biofumigant species being the main factor. Four species were included: *Brassica carinata* A.Braun (cv. Eleven), *Brassica juncea* L. (cv. Scala), *Raphanus sativus* L. (cv. Córdoba), and *Sinapis alba* L. (cv. Venice). Each elementary plot measured 10 m in length and 3.6 m in width, with a total area of 36 m^2.

Sowing took place on 22 September 2022 and 29 September 2023, using a 1.2 m wide experimental seeder. Seeding rates were 12.5 kg/ha for *B. carinata* and *B. juncea* and 25 kg/ha for *R. sativus* and *S. alba*. To promote germination in 2022, two emergency irrigations of 15 mm each were applied at the end of September and in early October. In 2023, rainfall during the same period was sufficient to ensure good germination, with an emergence rate of 75–80% for all species except *B. juncea*, which exhibited a rate of 32%. Given this low rate, germination and viability tests (tetrazolium test) were conducted, confirming that the low germination was not due to seed quality but to intrinsic characteristics of the species. Mineral fertilization in both growing cycles consisted of the application of 400 kg/ha of a complex N-P-K (S) 15-15-15 (13) fertilizer before sowing.

2.3. Analytical Determinations

In each elementary plot, various parameters were evaluated throughout the growth cycle of the biofumigant species, focusing on biomass production and distribution, as well as the physiological development of the plants. The determinations included:

Biomass Production: total biomass was quantified, distinguishing between the aboveground part and the roots, at different points during the cycle. For this, a 0.5 m^2 area (1 m × 0.5 m) from each elementary plot was manually harvested on the following dates: 23 January and 27 March 2023 (123 and 186 days after sowing (das), respectively) and 11 December 2023 and 29 January 2024 (73 and 122 das, respectively). After plant extraction, the roots were separated from the aboveground part for all plants, and fresh biomass was measured for both root and aboveground portions. A subsample of three representative plants was then selected, and the dry matter content of the root and aboveground biomass was determined separately after drying in a forced-air oven at 65 °C until a constant weight was achieved. By applying the dry matter content of the root and aboveground tissues to their respective fresh biomasses, root dry biomass (RDB) and aboveground dry biomass (ADB) were obtained, with the sum of these values representing the total dry biomass (TDB).

Glucosinolate extraction, purification, desulfatation, and analysis was carried out by the Instituto de Agricultura Sostenible (IAS-CSIC) following ISO Norm (1992) with some adaptations. In short, 50 mg of ground powder was placed in two 10 mL test tubes, to which

1.5 mL of 70% methanol and 100 µL of glucotropaeolin (5 mM and 20 mM, respectively), as internal standards (reference 89216; PhytoLab GmbH & Co. KG, Vestenbergsgreuth, Germany), were added. The tubes were kept in a water bath at 80 °C for GSL extraction. After 20 min at room temperature, the tubes were centrifuged at 3600 rpm for 20 min, and the supernatants were reserved for analysis.

For GSL purification, 96-well filter plates loaded with A25 DEAE Sephadex ion-exchange resin were prepared using a Millipore multiscreen column loader. A 150 µL quantity of 60% methanol was added to each well. After one hour, the liquid was removed with a vacuum pump. A 300 µL quantity of the sample supernatant was transferred to each well, and the liquid was again removed using the vacuum pump. After this, the wells were washed twice with 150 µL of 60% methanol and twice with water.

For enzymatic desulfatation of GSLs, 10 µL of water and 10 µL of sulfatase solution were added to each well, and the plates were kept overnight at room temperature. Desulfoglucosinolates were eluted by washing twice with 100 µL of 60% methanol and twice with water. The resulting collected samples containing desulfoglucosinolates were stored at −20 °C until analysis by HPLC.

The HPLC system consisted of a Waters 1525 binary pump, a Waters 2489 UV/visible detector set at 229 nm, and a Waters 2707 Autosampler (Waters Corporation, Milford, MA, USA). The column used was a Kinetex C18 of 250 × 4.6 mm, 100 Å ID, with a particle size of 5 µm (Phenomenex, Torrance, CA, USA). HPLC analysis was performed using water (solvent A) and 20% acetonitrile (solvent B) as eluents, with the following gradient: 2 min of solvent B at 0%, 23 min increasing solvent B to 100%, 5 min reducing solvent B back to 0%, and 5 min maintaining solvent B at 0%, at a flow rate of 1 mL/min and an oven temperature of 40 °C. Water quality was maintained at 18.2-megohm Milli-Q Direct Water (Merck Millipore, Darmstadt, Germany) for all analytical steps. Quantification of desulfoglucosinolates was carried out using response factors previously reported by ISO 9167 Norm [40] and Yi et al. (2016) [41] for GSLs not included in the ISO Norm. The GSLs analyzed are shown in Table 1.

Table 1. Nature and characteristics of the glucosinolates analyzed in the biomass of the biofumigant species.

Compound Type	Trivial Name	Chemical Name
Aliphatic	Epiprogoitrin	2(S)-Hydroxy-3-butenylglucosinolate
Aliphatic	Glucoalyssin	5-Methylsulfinylpentyl
Aliphatic	Glucobrassicanapin	4-Pentenyl
Aliphatic	Glucoerucin	4-Methylthiobutyl
Aliphatic	Glucoiberverin	3-Methylthiopropyl
Aliphatic	Gluconapin	3-Butenyl
Aliphatic	Glucoraphanin	4-Methylsulfinylbutyl
Aliphatic	Glucoraphasatin	4-Methylsulfanyl-3-butenyl
Aliphatic	Napoleiferin	5-Allyl-1,3-oxazolidin-2-thione
Aliphatic	Progoitrin	2-Hydroxy-3-butenyl
Aliphatic	Sinigrin	2-Propenyl
Aromatic	Gluconasturtiin	2-Phenylethyl
Aromatic	Glucotropaeolin	Benzyl
Aromatic	Sinalbin	4-hydroxybenzyl glucosinolate;
Indolyl	4-Hydroxyglucobrassicin	4-Hydroxy-3-indolylmethyl
Indolyl	Glucobrassicin	3-Indolylmethyl

The fraction of photosynthetically active radiation (PAR) intercepted by the canopy (fIPAR) was calculated as the ratio between intercepted PAR (incident PAR—transmitted PAR) and incident PAR, measured at solar noon on each sampling date, always under clear sky conditions. Based on the fIPAR values, the calculation of PAR intercepted by the

crop from sowing to each biomass sampling date was divided into as many sub-periods as there were fIPAR measurements. The intercepted PAR value for each sub-period was calculated by multiplying the incident PAR for that sub-period (daily incident PAR data were obtained from the meteorological station located near the trial site) by the arithmetic mean of the fIPAR values determined at the beginning and end of that sub-period.

In turn, RUE was calculated as an average RUE value for the period between the sowing date and each of the two biomass sampling dates for the biofumigant species. This was determined as the ratio between the TDB, in g of dry matter/m^2, and the amount of PAR intercepted by the canopy, in MJ/m^2, during the same time period. Thus, RUE, in g of dry matter/MJ, expresses the efficiency of the plant in converting intercepted radiation into biomass.

Chlorophyll content in the leaves of the biofumigant species was measured using a SPAD meter at different points in the growth cycle as an indicator of the plant's nutritional status. On each sampling date, 15 measurements were taken in each elementary plot (one leaf per plant from 15 plants) (Table 2).

Table 2. Parameters, equipment, and measurements carried out in the biofumigant species trial.

Parameter	Measurement Dates 2022/23 (das *)	Measurement Dates 2023/24 (das)	Equipment	Method/Procedure
Fraction of intercepted PAR (fIPAR)	22, 41, 67, 110, 123, 137, 161, 186		LI-191-R Quantum line sensor (LI-COR Environmental., Lincoln, NE, USA)	fIPAR = [Incident PAR − Transmitted PAR]/Incident PAR Transmitted PAR: average value of 3 measurements per elementary plot
SPAD	49, 70, 114, 138, 160, 174, 186.	122	SPAD-502® chlorophyll meter (Konica Minolta Inc., Tokyo, Japan)	Average value of 15 measurements (one leaf from 15 plants) per elementary plot and measurement date
Biomass produced: total, root, and aerial part	123, 186	73, 122	Precision balances EUROPE 600 and EUROPE 40000AR (Gibertini ©, Novate Milanese, MI, Italy) and drying oven 374 A (J.P Selecta S.A.U., Barcelona, Spain)	Sampled area per elementary plot: 0.5 m^2 (1 m × 0.5 m)
Glucosinolate concentration and types in the aerial part	123, 186	120, 190	Lyophilizer (Lyoquest 55 plus-Telstar), IKA A11 basic analytical mill (IKA-Werke GmbH & Co., KG., Staufen, Germany)	Leaf or root samples were frozen shortly after collection at −80 °C. The samples were lyophilized and maintained in a drying oven at 80 °C for 24 h for myrosinase inactivation and then ground.

(*): Days after sowing (das) date. Emergence (50% germination rate) occurred approximately 9 days after sowing.

2.4. Statistical Analysis

Analyses of variance of the biomass, fIPAR, RUE, SPAD, and GSL concentration were performed using Fisher's least significant difference (LSD) tests at 95.0% confidence. The tests were carried out using STATGRAPHICS Centurion XVIII statistical package software (StatPoint, Inc., Herndon, VA, USA). In order to estimate the correlation between the different parameters evaluated, the simple regression analysis was adjusted to the non-linear inverse-X model, as it showed the highest r^2 value.

3. Results

3.1. Agronomic Performance and Biomass Production

The field trial was repeated over two consecutive growing cycles, and in both cycles, significant differences were detected in the biomass produced by the biofumigant species analyzed. These differences and sampling variations were dependent on the growing cycle and the timing of the sampling (Table 3).

Table 3. Values and statistical analysis of total dry biomass (TDB) production parameters and its components (aboveground dry biomass—ADB and root dry biomass—RDB) for the biofumigant species in the two analyzed growing cycles.

Growing Cycle	1st Cycle (2022–23)						2nd Cycle (2023/24)					
Sampling Date	23 January 2023 (123 das)			27 March 2023 (186 das)			11 December 2023 (73 das)			29 January 2024 (122 das)		
Species	**ADB** [1]	**RDB** [1]	**TDB** [1]	**ADB** [1]	**RDB** [1]	**TDB** [1]	**ADB** [1]	**RDB** [1]	**TDB** [1]	**ADB** [1]	**RDB** [1]	**TDB** [1]
B. carinata	763.9 a[2]	73.1 a	837.0 a	576.4 ab	39.9 c	616.3 ab	315.0 b	73.1 c	388.1 b	515.6 a	85.3 b	600.9 a
B. juncea	642.5 a	124.8 a	767.3 a	735.3 a	92.1 ab	827.5 a	130.1 c	31.3 d	161.5 c	383.8 a	148.4 b	532.2 a
R. sativus	641.6 a	122.0 a	763.6 a	598.9 ab	131.4 a	730.3 ab	380.4 b	202.0 a	582.4 a	354.1 a	238.5 a	592.6 a
S. alba	647.2 a	67.4 a	714.7 a	493.5 b	56.5 bc	550.1 b	507.3 a	143.4 b	650.7 a	605.0 a	83.7 b	688.7 a
p value	ns [3]	ns	ns	*	**	*	***	***	***	ns	**	ns

[1] g of dry matter/m^2; [2] means followed by the same letter were not significantly different (ns) at $p \leq 0.05$ according to the Fisher's least significant difference (LSD); [3] *, **, *** and ns indicate significance at $p \leq 0.05$, 0.01, and 0.001 and non-significance at $p \leq 0.05$, respectively.

In the sampling conducted on 23 January 2023 (123 das), the four biofumigant species tested reached dry biomass production levels that did not differ significantly, either in total biomass or in its two components (root and aboveground). The values ranged from 837.0 g dry matter/m^2 for *B. carinata* to 714.7 g dry matter/m^2 for *S. alba* (Table 3). Furthermore, in all species, it was clear that the aboveground biomass contributed more significantly to the total dry biomass, representing between 84% and 91% of the total, depending on the species.

Approximately two months after the first sampling, and following a period of intense frost, the comparative analysis between the species showed changes in their ability to produce and accumulate biomass compared to what was observed in the 23 January sampling. In this second sampling, both the ADB and TDB produced by *B. juncea* were significantly higher than those produced by *S. alba*, with *B. carinata* and *R. sativus* falling in an intermediate position. This was a result of the minimal variations in biomass accumulation levels shown by *B. juncea* and *R. sativus* compared to the previous sampling, in contrast to the significant decrease experienced by *B. carinata* and *S. alba* (Table 3).

Consequently, although none of the four species appears to be well adapted to producing and accumulating biomass during periods of low temperatures (frost), it is evident that *B. carinata* and *S. alba* are extremely sensitive to such conditions (Table 3). This fact is crucial when determining the most appropriate timing for their incorporation into soil in regions where frosts occur.

The results obtained from the 2022 autumn sowing highlighted the need to adjust the sampling schedule for biomass determination in the 2023 autumn sowing (Table 3). The first biomass sampling was moved forward to 73 das (11 December 2023), while the second sampling remained at a similar date to the first cycle (around 120 das). This adjustment was based on the species' sensitivity to frost, aiming to assess their biomass production capacity in shorter cycles, concluding before the onset of the frost period. The decision was further supported by the noticeably higher initial growth rates of *R. sativus* and *S. alba*, as corroborated by their higher levels of PAR interception.

In the sampling conducted on 11 December 2023 (73 das), in terms of TDB, the four species were grouped into three levels with statistically significant differences: the first group consisted of *S. alba* and *R. sativus*, which surpassed *B. carinata* in TDB, and the latter, in turn, produced and accumulated more biomass than *B. juncea.* These results confirm the higher capacity of *S. alba* and *R. sativus* to produce biomass in short cycles (around 70 das), compared to the potential shown by *B. carinata* and, especially, by *B. juncea* at that stage.

As for the analysis of the two components that determine TDB (ADB and RDB), the key difference is that *S. alba* accumulates more biomass in the ADB than *R. sativus*, while in the RDB, the situation is reversed.

By the end of January 2024, 48 days after the previous sampling (122 das), the four biofumigant species reached very similar TDB values, in line with the results observed in the equivalent sampling from the 2022 autumn sowing trial. This is because *R. sativus* and *S. alba* maintained similar production levels to the previous sampling, showing virtually no growth during that period. In contrast, *B. carinata* and, particularly, *B. juncea* showed significant increases in TDB during that time, reaching levels comparable to the other two species (Table 3). Regarding the analysis of the two components (ADB and RDB), the most noteworthy observation is the greater accumulation of root biomass (RDB) in *R. sativus* compared to the other three species.

Having conducted homologous samplings in both trial growing cycles (approximately 120 das) for biomass determination in the four biofumigant species, a statistical analysis was performed using the results from both growing cycles, confirming the findings identified in the individual analyses from each trial growing cycle (Table 4).

Table 4. Values and statistical analysis of total dry biomass (TDB) and its components (aboveground dry biomass—ADB and root dry biomass—RDB) for the biofumigant species at 120 das across both growing cycles.

Sources of Variation	ADB [1]	RDB [1]	TDB [1]
B. carinata	639.8 a[2]	79.2 b	719.0 a
B. juncea	513.1 a	136.6 ab	649.7 a
R. sativus	497.8 a	180.2 a	678.1 a
S. alba	626.1 a	75.6 b	701.7 a
Species	ns [3]	*	ns
First	569.2 a	117.9 a	687.1 a
Second	464.6 b	139.0 a	603.6 b
Cycle	*	ns	*
Species × cycle	ns	ns	ns

[1] g of dry matter/m^2; [2] means followed by the same letter were not significantly different (ns) at $p \leq 0.05$ according to the Fisher's least significant difference (LSD); [3] * and ns indicate significance at $p \leq 0.05$ and non-significance at $p \leq 0.05$, respectively.

Although differences in biomass production were observed between the two growing cycles, particularly in terms of TDB, the general biomass distribution patterns remained consistent. *B. carinata* and *S. alba* showed a greater contribution of ADB to the TDB, while

R. sativus stood out for its accumulation of root biomass RDB. Furthermore, the differences in production efficiency between the cycles reinforce the idea that climatic conditions and the duration of the cycle significantly influence the final performance of the biofumigant species. Nevertheless, the consistent behavior of the species in terms of biomass distribution suggests that management strategies, such as the timing of incorporation into the soil, should be adjusted according to these patterns. The results confirm that all species are capable of reaching similar levels of biomass accumulation, but with significant differences in how they allocate resources between the aboveground portion and the root, which is a key factor to consider when implementing biofumigation strategies.

3.2. Radiation Interception and Radiation Use Efficiency

3.2.1. Fraction of Photosynthetically Active Radiation Intercepted by the Canopy (fIPAR)

The evolution of fIPAR by the different biofumigant species throughout the 2022–23 agronomic cycle underwent significant variations (Figure 2).

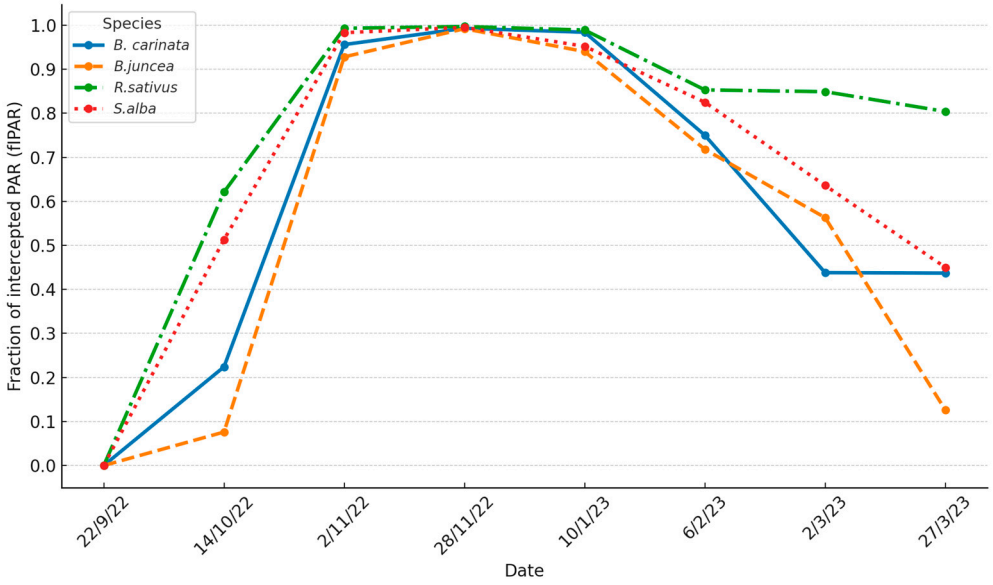

Figure 2. Evolution of the fraction of photosynthetically active radiation intercepted by the canopy (fIPAR) of the biofumigant species throughout the 2022–23 cycle.

The main differences in the evolution of fIPAR between the biofumigant species occurred in the initial and final stages of the 2022–23 cycle. In the initial stage (22 das), *R. sativus* and *S. alba* had higher fIPAR values than *B. carinata* as a result of more vigorous early germination and growth. In turn, *B. carinata* showed higher fIPAR values than *B. juncea*.

As the cycle progressed, these initial differences between the species gradually decreased. By early November 2022 (41 das), only *B. juncea* showed lower PAR interception levels compared to the other species, which had already reached fIPAR values above 0.95. By the end of November 2022 (67 das) (Figure 2), fIPAR values approached 1 (between 0.99 and 1) in all four species.

The frost period began in late November 2022 (Figure 3) with three days of mild frost (minimum temperature ≥ -1.7 °C). In December 2022 and the first half of January 2023, there were almost no frosts, and all four species continued to show very high fIPAR levels. However, in the last ten days of January 2023, much of February, and the first week of March 2023, the crop was subjected to a prolonged frost period (45 frost days, of which 25 days had minimum temperatures below -2 °C, with some days reaching as low as -8 °C).

Figure 3. Image of the biofumigant species trial on 22 November 2022 (67 das).

As a result, by the end of January 2023, the species began to experience a decline in soil coverage or canopy shading, which was reflected in their fIPAR values. This decline was more pronounced in *B. carinata*, *B. juncea*, and *S. alba* compared to *R. sativus*. The process worsened in the following months, such that by early March, fIPAR values had dropped to around 0.5–0.6 for the first three species, while *R. sativus* maintained an fIPAR of around 0.85. This species was able to "renew and maintain" its canopy through continuous regrowth of the shoot, fueled by reserves stored in the roots.

3.2.2. PAR Intercepted During the Cycle and Radiation Use Efficiency

The integrated effect of the evolution of fIPAR was reflected in the total values of PAR intercepted by each of the biofumigant species from sowing until each of the two biomass sampling dates (123 and 186 das) (Figure 4).

On the two analyzed dates, statistically significant differences were observed in the overall values of intercepted PAR between the species, with a similar general pattern in both cases. The RUE, a coefficient that indicates how the intercepted or absorbed PAR is used by the crop for biomass production, is known to vary based on multiple factors, including environmental stresses, phenological stages, genotypes [42], water and nitrogen availability [43], species, crop management, weather conditions [44], and plant density [39], as well as the interactions between these factors [42]. *R. sativus* and *S. alba* intercepted a greater amount of PAR due to faster initial growth and development compared to *B. carinata*, which in turn surpassed *B. juncea* in intercepted PAR. This is primarily the result of poorer and more irregular germination and slower initial growth in *B. juncea*. The only notable difference in the comparative analysis between species on both dates is that in the late March sampling (186 das), *R. sativus* intercepted more PAR than *S. alba*, as *R. sativus* was able to maintain a greater green foliar cover during the frost period.

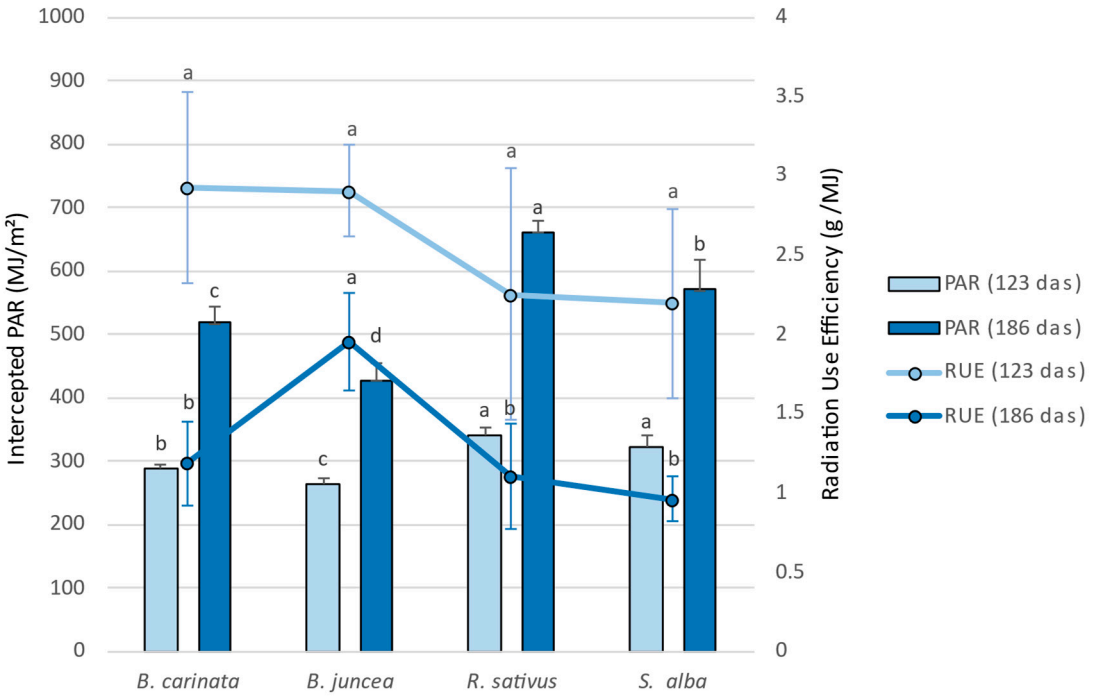

Figure 4. Intercepted photosynthetically active radiation (PAR) (MJ/m^2) and radiation use efficiency (RUE) (g/MJ) by the foliar cover of the biofumigant species on two dates (123 and 186 das). Means followed by the same letter were not significantly different (ns) at $p \leq 0.05$ according to Fisher's least significant difference (LSD).

Regarding the RUE values at 123 das, no statistically significant differences (5% significance level) were observed among the different biofumigant species, although both *R. sativus* and *S. alba* showed slightly lower average values compared to the other two species. Therefore, there seems to be a clear compensatory effect between the two factors that determine biomass production (RUE and intercepted PAR), which explains why there are no statistically significant differences in accumulated biomass production up to that date among the four tested species. In line with previous studies, *Brassica* species tend to cover the soil rapidly, resulting in high radiation capture (517 MJ/m^2), although their radiation use efficiency remains low (0.80 g/MJ) when compared to other cover crops [18].

Considering a cycle of 186 das, *B. juncea* reaches much higher RUE values compared to the other three species (Figure 4), with highly significant differences between the two groups. It is noteworthy that all four species show a decline in RUE due to greater foliar cover senescence, partly caused by the extended cycle through the end of winter and partly by the frost period they experienced during much of the winter. In any case, *B. juncea* exhibited the smallest decline in RUE. Once again, the integrated analysis of both parameters (intercepted PAR and RUE) perfectly explains the differences observed in biomass production among the different biofumigant species in the late winter sampling (186 das). *B. juncea* is the species with the highest biomass production (with statistically significant differences compared to *S. alba*), as its lower capacity to intercept PAR—due to reduced growth under low-temperature conditions—is compensated by higher RUE values. In the case of *R. sativus*, the lower biomass production is attributed to its low RUE, not the amount of intercepted PAR. For the remaining two species (*B. carinata* and *S. alba*), the lower biomass accumulation is due to both a decrease in intercepted PAR and in RUE, which indicates that these two species are the most affected by low-temperature conditions in terms of biomass production and accumulation.

Furthermore, in the analysis of the correlations between accumulated biomass and the two factors that determine it (intercepted PAR and RUE), in both samplings (123 and 186 das), it is evident that the relationship between biomass and RUE is much stronger than that between biomass and intercepted PAR (Figure 5).

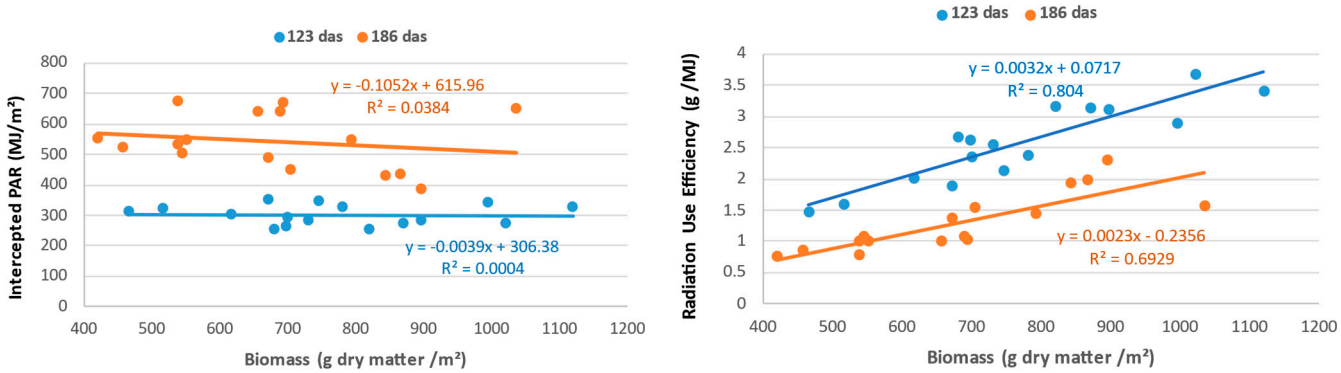

Figure 5. Analysis of the relationships between accumulated biomass at 123 and 186 days after sowing (das) and its determining components: intercepted photosynthetically active radiation (PAR) (**left**) and radiation use efficiency (RUE) (**right**).

3.3. Chlorophyll Content Index

On the first three SPAD measurement dates, corresponding to the period of the cycle during which frost had barely occurred (up until 13 January 2023), the statistical analysis of the results reveals that the four biofumigant species were grouped into two distinct categories with significant differences between them. The first group consisted of *B. carinata* and *B. juncea*, with SPAD values ranging from approximately 36.9 to 38.9, while the second group included *R. sativus* and *S. alba*, with SPAD values between approximately 30.4 and 33.6 (Table 5).

Table 5. Values and statistical analysis of the SPAD of biofumigant species on different sampling dates throughout the 2022–23 and 2023–24 cycles.

Sampling Date	10 November 2022	1 December 2022	13 January 2023	6 February 2023	1 March 2023	29 January 2024
B. carinata	36.9 a[1]	37.2 a	38.1 a	40.5 a	13.2 c	38.7 a
B. juncea	37.3 a	36.0 ab	38.9 a	37.4 ab	20.0 b	40.3 a
R. sativus	31.1 b	31.2 c	30.4 b	33.0 b	30.9 a	29.1 b
S. alba	33.6 ab	33.1 bc	32.9 b	25.2 c	12.7 c	29.8 b
p-value	*[2]	*	***	***	***	***

[1] Means followed by the same letter were not significantly different (ns) at $p \leq 0.05$ according to the Fisher's least significant difference (LSD); [2] *, and *** indicate significance at $p \leq 0.05$, and 0.001, respectively. In the data collection from early February 2023, the most notable difference compared to the previous observations is the significant decrease in SPAD experienced by *S. alba*, which became statistically distinct from the SPAD values of *R. sativus*.

Finally, in early March 2023, after enduring a prolonged period of low temperatures, the differences in SPAD values among the biofumigant species became much more pronounced. This was due to the sharp decline in SPAD values observed in *B. carinata*, *B. juncea*, and *S. alba*, a trend not observed in *R. sativus*, which either maintained or only slightly decreased its SPAD values compared to previous measurements. As a result, at that time, the four biofumigant species grouped into three distinct levels with highly significant differences between them.

During the winter of the second sowing cycle (2023–2024), SPAD was measured on 29 January 2024 (122 das). The results obtained on this date confirm a similar trend to

that observed in the previous cycle (2022–23), both in absolute SPAD values and in the significant differences among the biofumigant species.

In this cycle, *B. juncea* showed the highest SPAD values, with a mean of 40.3 ± 2.6. These values are consistent with the results of the previous cycle, where *B. juncea* also exhibited high values, reflecting a strong ability to maintain elevated chlorophyll levels in its leaves. *B. carinata* also recorded high SPAD values, with a mean of 38.7 ± 1.1, suggesting a consistent trend for this species regarding the SPAD parameter.

In contrast, *R. sativus* and *S. alba* displayed significantly lower SPAD values, with mean SPAD values consistently below 30. This difference between groups is in line with observations from the previous cycle, where both species also presented lower SPAD values compared to *B. carinata* and *B. juncea*.

These results reinforce the hypothesis that SPAD is strongly influenced by biofumigant species, highlighting the importance of further investigating the relationship between this parameter and other key factors, such as the concentration of GSLs, which may contribute to the biofumigant potential of the species.

3.4. Glucosinolate Profiles and Isothiocyanate Potential

The GSL profiles in the *Brassica* species analyzed during January and March of 2023 and 2024 showed a marked differentiation between aliphatic, aromatic, and indolic types, with significant variations in concentration among species (Figure 6). Specifically, *B. juncea* exhibited the highest overall GSL concentration in both cycles and across months, with the values in January being notably higher than those in March. *S. alba* also presented high GSL levels, particularly in the second cycle's March sample, where it reached its peak concentration. In contrast, *B. carinata* and *R. sativus* demonstrated comparatively lower GSL concentrations, with *B. carinata* showing a substantial decrease from January to March, especially in the second cycle, suggesting seasonal or environmental influences on GSL biosynthesis.

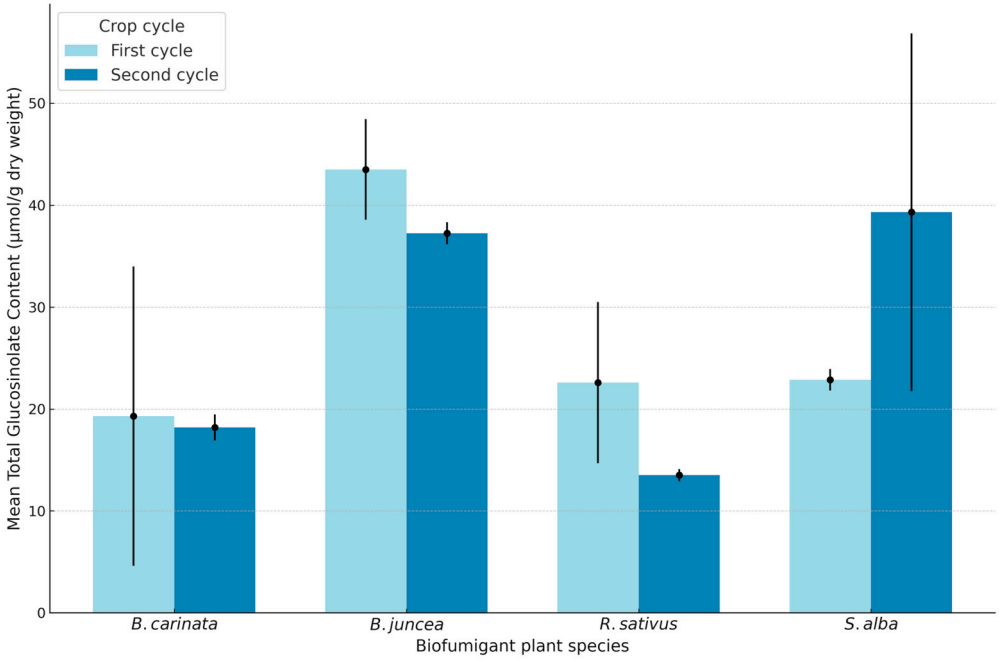

Figure 6. Total glucosinolate concentration in biofumigant plant species during the first and second cycles (January and March sampling).

Figure 6 illustrates these trends, where *B. juncea* and *S. alba* consistently dominate in GSL levels, potentially highlighting their enhanced metabolic capacity for GSL synthesis

under varying conditions. The differences between cycles, represented by varying shades of blue, underscore potential annual environmental impacts or adaptations, as the second cycle showed slightly reduced concentrations for *B. juncea* in March, while *S. alba* reached its maximum in that period. These fluctuations point to species-specific responses to environmental variables, possibly due to differences in genetic regulation of GSL pathways. The visual separation of values by month and cycle further emphasizes the importance of timing and environmental context in GSL concentration and composition among *Brassica* species (Figures 6 and 7).

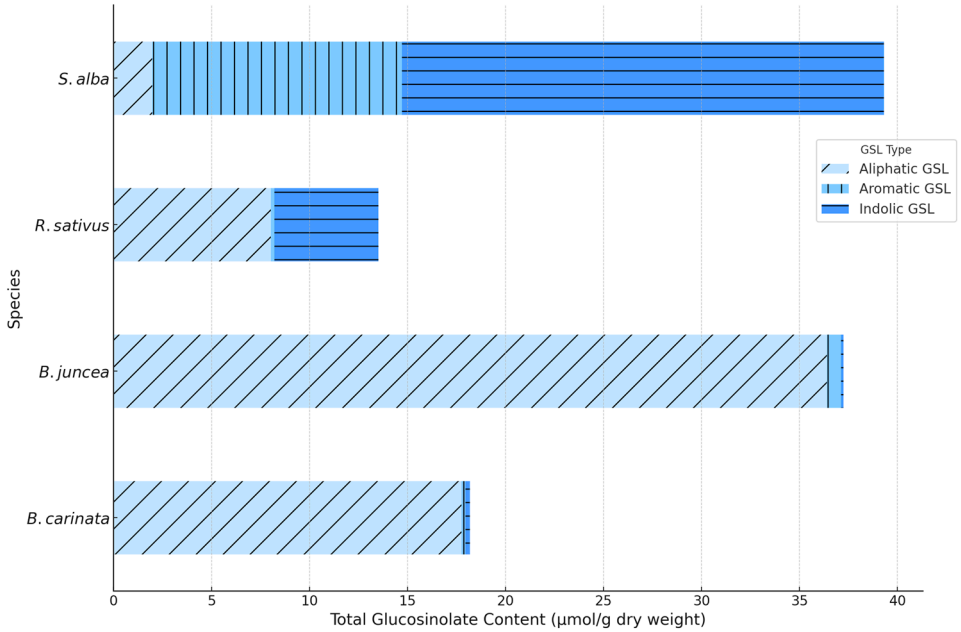

Figure 7. Comparison of aliphatic, aromatic, and indolic glucosinolate concentration in biofumigant plant species: 2023–2024.

Figure 7 shows that aliphatic GSLs exhibited the highest concentrations in most species in both growing cycles, with sinigrin standing out as a key compound in *B. juncea* and *B. carinata*, known for releasing ITCs with fungicidal effects. Among these, sinigrin was one of the most predominant aliphatic compounds. Other notable aliphatic GSLs included glucoraphanin and glucoerucin, which produce ITCs such as sulforaphane and erucin, respectively, compounds with well-known effects on plant defense.

Additionally, gluconapin and glucotropaeolin contributed to the aliphatic profile in lower concentrations, with hydrolysis products such as benzyl isothiocyanate [33]. Between January and March, aliphatic GSLs decreased by an average of 15–20% in these species, particularly in *B. juncea*, which could indicate an early defensive adjustment.

In contrast, aromatic GSLs, primarily sinalbin in *S. alba*, were more stable over the two growing cycles of analysis, showing a less seasonally dependent profile.

Regarding aromatic GSLs, sinalbin and gluconasturtiin were notable for their presence, with major products such as nitriles and phenethyl isothiocyanates. In *R. sativus*, indolic GSLs were significantly concentrated in January, showing reductions of up to 25% by March (Figure 7). Between the growing cycles, there was a trend of stability in aromatic GSLs and a slight reduction in aliphatic GSLs in 2024, particularly in March, suggesting an interannual adaptation in the defensive response of these species to environmental factors.

3.5. Correlation Analysis of Measured Variables

As highlighted in the previous section, the concentrations and profiles of GSLs show clear differences between the tested species, which indicates their likely different biofu-

migant effects. These differences are much greater than those observed in the amounts of biomass produced by the species in 120-day cycles, suggesting that the differences in the total amounts of GSLs incorporated into the soil by the end of their cycle will largely depend on their GSL concentration. The precise determination of these concentration and profiles requires labor-intensive sampling, treatment, and preservation procedures, as well as costly analytical determinations. Therefore, it is of great interest to analyze the potential relationships between crop indicators (biofumigant species) that are quick and easy to measure through proximal and/or remote sensors, and GSL concentration is a tool to assist in decision-making regarding the optimal point in the cycle for incorporating biofumigant species biomass into the soil. One of these quick and easy-to-measure indicators is the SPAD.

Figure 8 graphically shows the relationship between the total GSL concentration in the biomass of the biofumigant species and the SPAD from the samples taken in January and March 2023. In the January 2023 sampling, this relationship is consistent (r^2 = 0.74), exhibiting an exponential relationship: the higher the SPAD, the higher the GSL concentration.

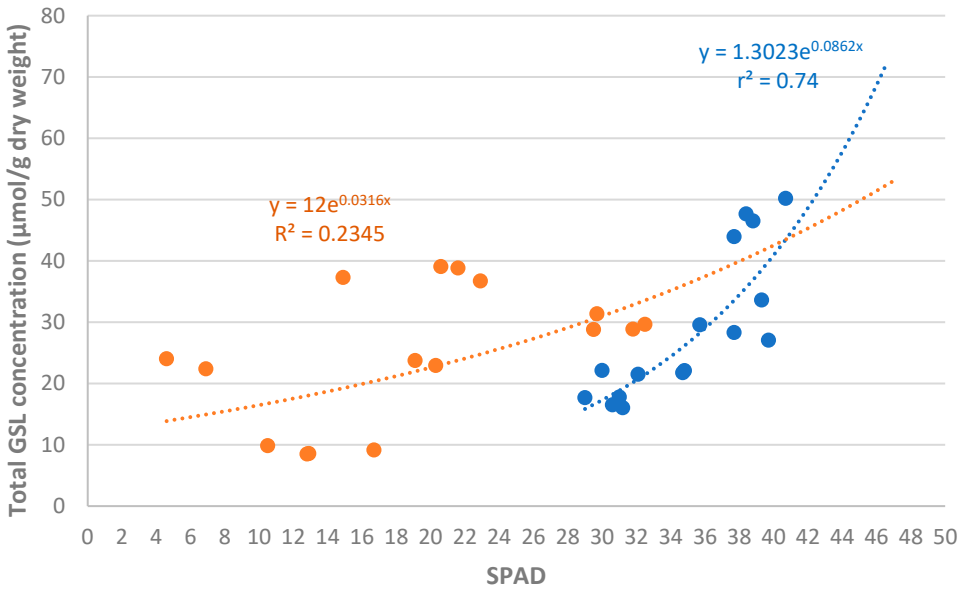

Figure 8. Individual analysis of the relationship between total glucosinolate concentration in the biomass of biofumigant species and the SPAD values in the January (blue) and March (red) 2023 samplings.

In the March 2023 sampling, however, the relationship is much less consistent (r^2 = 0.23). It is very likely that the frosts occurring between the two samplings, which strongly affected the SPAD of the species, were the most determining factor in the loss of consistency in this relationship.

As mentioned, SPAD values and GSL concentration and profiles appear to be strongly dependent on or linked to species. However, many other environmental and agronomic management factors affect both parameters. In this regard, when analyzing results from multiple years, it is necessary to express the results in relative terms compared to a reference to eliminate the effect of additional sources of variation that may distort the analysis of this relationship. In this case, *B. juncea* was chosen as the reference species, as it showed the highest GSL concentration and, along with *B. carinata*, was also among the species with the highest SPAD values.

The global analysis of this relationship, corresponding to the January 2023 and 2024 samplings (Figure 9), shows a very similar consistency (r^2 = 0.71) to that obtained in the individual analysis of January 2023 (Figure 8). This opens up interesting possibilities for

further investigation into this relationship and its consideration as a practical tool in the implementation of biofumigation strategies.

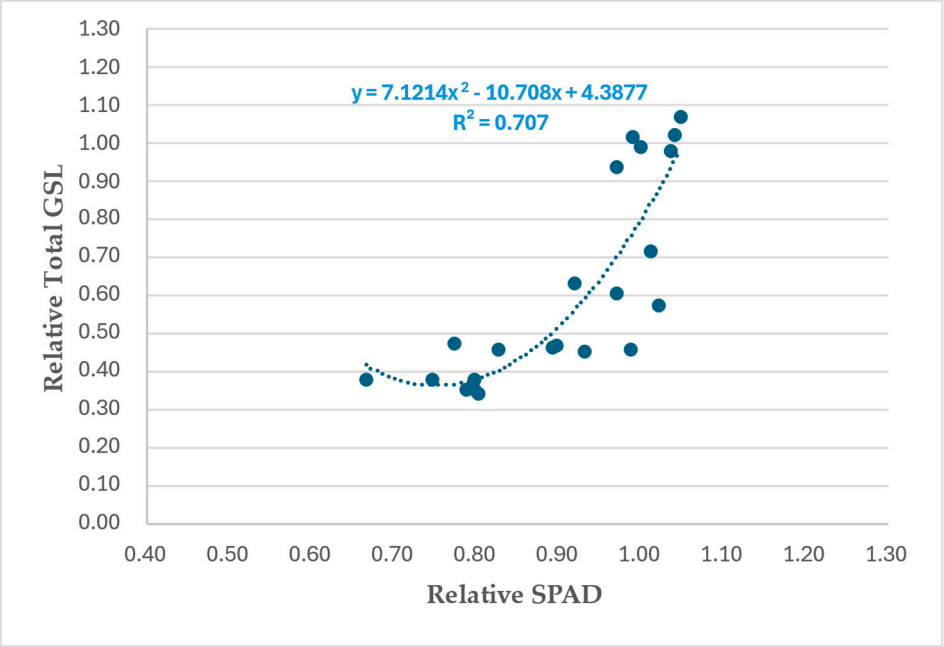

Figure 9. Global analysis of the relationship between relative total glucosinolate concentration in the biomass of biofumigant species and the relative SPAD values in the January 2023 and 2024 samplings (120 das).

4. Discussion

The biomass production of *S. alba* and *R. sativus* observed in our study was substantially higher than the values reported by Brant et al. (2011) [17], who recorded values between 115.8 and 138.2 g/m^2 for these species during summer–autumn cycles under water-limited conditions. However, our biomass production values were similar to the values shown by Elhakeem et al. (2021) [18] for these species during summer–autum cycles under Northern European conditions.

Differences can be attributed to lower water deficits and more favorable conditions for radiation use efficiency (RUE). Nevertheless, the three studies highlight the rapid growth rates of *S. alba* and *R. sativus* during the initial phases of their growth cycles, reinforcing their suitability for biofumigation applications.

The radiation capture (PAR) observed in this study for *R. sativus* and *S. alba* over a 120-day cycle (320–340 MJ/m^2) (Figure 4) was higher than values by Elhakeem et al. (2021) [18] (233 MJ/m^2), despite their earlier sowing date. This can be explained to differences in cycle duration (84 days vs. 120 days) and climatic conditions. Similarly, the RUE values were comparable, with our study reporting 2.2 g/MJ (total biomass) versus their adjusted value of 1.87 g/MJ.

RUE values observed for *B. carinata*, *B. juncea*, and *B. napus* were notably higher than those reported by Kuai et al. (2016) [39] for *B. napus*. This difference can be attributed to the higher sowing densities used in our trial and the shorter cycle duration. These findings suggest that denser planting schemes and seasonality significantly enhance biomass production efficiency in biofumigant species.

Our results support previous findings that show RUE as a more determinant factor for biomass production than PAR interception alone, particularly under varied environmental conditions and crop management approaches [42]. Ultimately, RUE better explains the biomass production capacity of the four tested biofumigant species than intercepted PAR.

While significant differences between the biofumigant species became evident in the second sampling date of the first cycle, particularly in aboveground biomass, the second cycle shows consistency in species with higher initial growth rates, such as *S. alba* and *R. sativus*. The aboveground biomass of *B. carinata*, measured at the mid-flowering stage, according to [38], ranged between 435 and 2417 g/m^2, with *S. alba* and *B. juncea* at 140–387 g/m^2 and 205–1792 g/m^2, respectively, reinforcing these species' significant biomass yield potential. These two species again outperformed *B. juncea* and *B. carinata* in biomass accumulation during the early samplings. This consistency across both cycles confirms that *S. alba* and *R. sativus* are more efficient at producing biomass in the early stages of cultivation, making them better suited for short cycles, such as those ending before frosts. Despite variation in biomass production, GSL concentration within plant tissues is largely genetically determined but is also influenced by factors such as plant organs, developmental stage, and environmental conditions [19,31,38,45,46]. On the other hand, *B. juncea* and *B. carinata*, although initially showing slower growth, managed to catch up with the other species in the later stages of the cultivation cycle, suggesting a compensatory ability under more extended conditions.

Thus, the results from both cycles highlight the importance of tailoring the choice of biofumigant species to the duration of the cultivation cycle and specific climatic conditions, with particular attention to the sensitivity of some species to low temperatures. This selection process should also take into account biofumigant characteristics beyond GSL concentration, such as biomass yield, adaptability to specific environmental conditions, and the species' ability to release bioactive compounds like ITCs, as demonstrated in studies by do Santos et al. (2021) [3].

While this study is focused on the specific conditions of central Spain, the potential applicability of the results to production systems in Northern Europe warrants consideration. Northern Europe presents different climatic conditions, such as cooler temperatures, higher rainfall, and shorter growing seasons, which could significantly influence the growth, biomass production, and glucosinolate (GSL) profiles of biofumigant species. For instance, the frost sensitivity observed in *B. carinata* and *S. alba* in this study suggests that these species might require careful timing of sowing and incorporation to avoid frost damage. Conversely, the robust early growth and biomass production of *R. sativus* and *S. alba* could make them suitable candidates for shorter cycles in regions with limited growing seasons.

The results of this study underscore the potential efficacy of *Brassica* species as biofumigants, particularly those with high levels of aliphatic GSLs, such as sinigrin in *B. juncea* and *B. carinata*. According to Sarwar et al. (1998) [47], aliphatic GSLs are notably effective due to their ability to release volatile ITCs, which exhibit broad-spectrum toxicity against fungal pathogens and nematodes [38]. Our results show that aliphatic GSL concentrations were highest in these species during the January analysis, suggesting an adaptive strategy to maximize the release of bioactive compounds in the early growth stages. In fact, aliphatic GSLs such as sinigrin (0.1–26.5 and 10.0–20.0 µmol/g in *B. juncea* and *B. carinata*, respectively), whose main product is allyl isothiocyanate, known for its bioactive properties [21], have been shown by other authors [38,48] to dominate the aboveground biomass in these species, contributing to their higher biofumigation efficacy [37,38]. Additionally, the high levels of aliphatic GSLs in *B. juncea* and *B. carinata* indicate that their biofumigant potential could still be also effective under Northern European conditions, provided that these species are managed to optimize growth before the onset of adverse weather. Future research evaluating these species under different environmental conditions is necessary to validate their performance and biofumigation efficacy in diverse European production systems.

Similarly, aromatic GSLs, such as sinalbin in *S. alba*, showed less variability between sampling dates, aligning with the findings of Torrijos et al. (2023) [48] and our observations of sinalbin stability from January to March. This suggests that aromatic GSLs play a more consistent defensive role, particularly against less volatile threats like insects [49]. Unlike aliphatic GSLs, sinalbin primarily produces nitriles instead of ITCs [26,47], indicating a complementary function with fewer direct fungicidal effects. The constant levels of sinalbin in *S. alba* highlight its role in defending against pathogens or environmental stressors where a steady presence is advantageous. However, despite their high toxicity in controlled laboratory conditions [25,33], aromatic GSLs are less effective for soil biofumigation due to their lower volatility and stronger sorption to organic matter, limiting their use in field applications [24,50].

Indolic GSLs, such as glucobrassicin, although not releasing ITCs, offer indirect benefits by inducing defense responses in host plants, including the activation of auxins and related signaling compounds [35,38]. In *R. sativus*, the intermediate levels of indolic GSLs observed in January may reflect early-stage adaptations to abiotic stress. These compounds, including glucobrassicin and 4-hydroxyglucobrassicin, release hydrolysis products like indoles [26], which serve critical defensive functions against herbivores and as signaling molecules in response to tissue damage, rather than providing direct fungicidal effects. This could suggest a strategic defensive adaptation, with indolic compounds being more abundant in early growth stages when abiotic stresses are more pronounced and decreasing later in the growing cycle.

Among the species studied, *B. juncea* demonstrated the most robust aliphatic GSL profile, followed by *B. carinata*, reinforcing its potential for biofumigation strategies targeting stronger fungicidal effects. Conversely, *R. sativus* displayed a more mixed profile, combining aliphatic and indolic GSLs. This diversity could be advantageous in environments with a broader range of pathogens and highlights its utility in rotational biofumigation practices with varying GSL profiles.

These findings underscore the importance of considering both seasonal and interannual variations in GSL profiles when developing *Brassica*-based biofumigation strategies. Tailoring these strategies to specific environmental challenges and seasonal dynamics will be critical to optimizing their efficacy.

5. Conclusions

This comprehensive evaluation of *Brassicaceae* species for biofumigation reveals significant species-specific variations that are crucial for optimizing biofumigation strategies. Results highlight the potential of using the SPAD values as an indirect estimator, at least in relative terms, of total GSL concentration in the biomass of these four biofumigant species, serving as a tool to aid in the practical implementation of biofumigation. The need to use a reference species may present a "minor" practical inconvenience, but it is advisable whenever working with crop indicators, whose absolute values depend on many uncontrollable variables. Additionally, these results also open the door to exploring other crop indicators of different types: chlorophyll-related indicators, such as normalized difference red edge (NDRE) index; vegetative development indicators, such as normalized difference vegetation index (NDVI) and green normalized difference vegetation (GNDVI); and combined indices such as transformed chlorophyll absorption in reflectance index/optimized soil-adjusted vegetation index (TCARI/OSAVI), determined using remote sensors (multispectral cameras mounted on drones, satellite imagery). These indicators hold great potential for application on a larger scale (large plots) compared to the SPAD measurements obtained with portable reflectometers.

Author Contributions: Conceptualization, J.M.A. and D.P.; methodology, J.M.A. and J.S.; software, J.S.; validation, R.L. and D.P.; formal analysis, J.M.A. and D.P; investigation, J.M.A. and D.P.; resources, D.P.; data curation, J.M.A.; writing—original draft preparation, D.P. and J.M.A.; writing—review and editing, R.L.; visualization, J.M.A. and D.P.; supervision, J.M.A.; project administration, D.P.; funding acquisition, D.P. All authors have read and agreed to the published version of the manuscript.

Funding: This research was funded by the Plan Estatal de Investigación Científica, Técnica y de Innovación 2021–2023 and Proyectos de Generación de Conocimiento, Convocatoria 2021 (PID2021-125545OR-C22).

Institutional Review Board Statement: Not applicable.

Data Availability Statement: The data presented in this study are openly available in e-cienciaDatos (publicly accessible repository) at https://doi.org/10.21950/0UHHSU.

Conflicts of Interest: The authors declare no conflict of interest.

References

1. Billen, G.; Aguilera, E.; Einarsson, R.; Garnier, J.; Gingrich, S.; Grizzetti, B.; Lassaletta, L.; Le Noë, J.; Sanz-Cobena, A. Beyond the Farm to Fork Strategy: Methodology for Designing a European Agro-Ecological Future. *Sci. Total Environ.* **2024**, *908*, 168160. [CrossRef] [PubMed]
2. Brennan, R.J.B.; Glaze-Corcoran, S.; Wick, R.; Hashemi, M. Biofumigation: An Alternative Strategy for the Control of Plant Parasitic Nematodes. *J. Integr. Agric.* **2020**, *19*, 1680–1690. [CrossRef]
3. dos Santos, C.A.; de Souza, A.C.; Ferreira, M.G. Biofumigation with Species of the *Brassicaceae* Family: A Review. *Cienc. Rural.* **2021**, *51*, 1–17. [CrossRef]
4. Chekanai, V.; Neilson, R.; Clark, M.; Edwards, S.G.; Roberts, D.; Back, M. Management of and Future Perspectives on Plant Parasitic Nematodes Associated with Narcissus Grown in the UK. *J. Hortic. Sci. Biotechnol.* **2024**, *100*, 1–10. [CrossRef]
5. Kirkegaard, J.A.; Gardner, P.A.; Desmarchelier, J.M.; Angus, J.F. Biofumigation—Using *Brassica* Species to Control Pests and Diseases in Horticulture and Agriculture. In Proceedings of the 9th Australian Research Assembly on Brassicas, Wagga Wagga, Australia, 5–7 October 1993; Wratten, N., Mailer, R.J., Eds.; Agricultural Research Institute: Wagga Wagga, Australia, 1993; pp. 77–82.
6. Dutta, T.K.; Khan, M.R.; Phani, V. Plant-Parasitic Nematode Management via Biofumigation Using *Brassica* and Non-*Brassica* Plants: Current Status and Future Prospects. *Curr. Plant Biol.* **2019**, *17*, 17–32. [CrossRef]
7. Karavina, C.; Mandumbu, R. Biofumigation for Crop Protection: Potential for Adoption in Zimbabwe. *J. Anim. Plant Sci.* **2012**, *14*, 1996–2005.
8. Lazzeri, L.; Malaguti, L.; Cinti, S.; Ugolini, L.; De Nicola, G.R.; Bagatta, M.; Casadei, N.; D'Avino, L.; Matteo, R.; Patalano, G. The *Brassicaceae* Biofumigation System for Plant Cultivation and Defence. An Italian Twenty-Year Experience of Study and Application. *Acta Hortic.* **2013**, *1005*, 375–382. [CrossRef]
9. Ntalli, N.; Caboni, P. A Review of Isothiocyanates Biofumigation Activity on Plant Parasitic Nematodes. *Phytochem. Rev.* **2017**, *16*, 827–834. [CrossRef]
10. Wei, F.; Passey, T.; Xu, X. Effects of Individual and Combined Use of Bio-Fumigation-Derived Products on the Viability of *Verticillium Dahliae* Microsclerotia in Soil. *Crop Prot.* **2016**, *79*, 170–176. [CrossRef]
11. Goswami, B.; Pariyar, B. Biofumigation-a Sustainable Alternative to Chemical Control of Soil Borne Pathogens: A Review. *Int. J. Adv. Multidiscip. Res. Stud.* **2024**, *4*, 134–138.
12. Gamliel, A.; van Bruggen, A.H.C. Maintaining Soil Health for Crop Production in Organic Greenhouses. *Sci. Hortic.* **2016**, *208*, 120–130. [CrossRef]
13. Céspedes, C.L.; Avila, J.G.; Martínez, A.; Serrato, B.; Calderón-Mugica, J.C.; Salgado-Garciglia, R. Antifungal and Antibacterial Activities of Mexican Tarragon (*Tagetes lucida*). *J. Agric. Food Chem.* **2006**, *54*, 3521–3527. [CrossRef] [PubMed]
14. Barros, A.F.; Campos, V.P.; da Silva, J.C.P.; Pedroso, M.P.; Medeiros, F.H.V.; Pozza, E.A.; Reale, A.L. Nematicidal Activity of Volatile Organic Compounds Emitted by *Brassica Juncea*, *Azadirachta Indica*, *Canavalia Ensiformis*, *Mucuna Pruriens* and *Cajanus* Cajan against *Meloidogyne Incognita*. *Appl. Soil Ecol.* **2014**, *80*, 34–43. [CrossRef]
15. Arnault, I.; Fleurance, C.; Vey, F.; Fretay, G.D.; Auger, J. Use of Alliaceae Residues to Control Soil-Borne Pathogens. *Ind. Crops Prod.* **2013**, *49*, 265–272. [CrossRef]
16. Wieczorek, R.; Zydlik, Z.; Zydlik, P. Biofumigation Treatment Using *Tagetes Patula*, *Sinapis Alba* and *Raphanus Sativus* Changes the Biological Properties of Replanted Soil in a Fruit Tree Nursery. *Agriculture* **2024**, *14*, 1023. [CrossRef]

17. Brant, V.; Pivec, J.; Fuksa, P.; Neckář, K.; Kocourková, D.; Venclová, V. Biomass and Energy Production of Catch Crops in Areas with Deficiency of Precipitation during Summer Period in Central Bohemia. *Biomass Bioenergy* **2011**, *35*, 1286–1294. [CrossRef]
18. Elhakeem, A.; van der Werf, W.; Bastiaans, L. Radiation Interception and Radiation Use Efficiency in Mixtures of Winter Cover Crops. *Field Crops Res.* **2021**, *264*, 108034. [CrossRef]
19. Morris, E.K.; Fletcher, R.; Veresoglou, S.D. Effective Methods of Biofumigation: A Meta-Analysis. *Plant Soil* **2020**, *446*, 379–392. [CrossRef]
20. Matthiessen, J.; Kirkegaard, J. Biofumigation and Enhanced Biodegradation: Opportunity and Challenge in Soilborne Pest and Disease Management. *CRC Crit. Rev. Plant Sci.* **2006**, *25*, 235–265. [CrossRef]
21. Hanschen, F.S.; Winkelmann, T. Biofumigation for Fighting Replant Disease-a Review. *Agronomy* **2020**, *10*, 425. [CrossRef]
22. Kirkegaard, J. Biofumigation for Plant Disease Control—From the Fundamentals to the Farming System. In *Disease Control in Crops: Biological and Environmentally Friendly Approaches*; Walters, D., Ed.; Wiley-Blackwell: Oxford, UK, 2009; pp. 172–195.
23. Fahey, J.W.; Zalcmann, A.T.; Talalay, P. The Chemical Diversity and Distribution of Glucosinolates and Isothiocyanates among Plants. *Phytochemistry* **2001**, *56*, 5–51. [CrossRef] [PubMed]
24. Clarkson, J.; Michel, V.; Neilson, R. Biofumigation for the Control of Soil-Borne Diseases. Soil Borne Disease Focus Group 2015. Available online: https://ec.europa.eu/eip/agriculture/sites/default/files/9_eip_sbd_mp_biofumigation_final_0.pdf (accessed on 1 November 2024).
25. Chekanai, V.; Neilson, R.; Roberts, D.; Edwards, S.; Back, M. In Vitro Nematicidal Efficacy of *Brassica*-Derived Isothiocyanates against the Root Lesion Nematode, *Pratylenchus Penetrans*. *Nematology* **2024**, *26*, 899–908. [CrossRef]
26. Agerbirk, N.; Olsen, C.E. Glucosinolate Structures in Evolution. *Phytochemistry* **2012**, *77*, 16–45. [CrossRef] [PubMed]
27. Rosa, E.A.S.; Heaney, R.K.; Fenwick, G.R.; Portas, C.A.M. Glucosinolate in Crop Plants. In *Horticultural Reviews*; Janick, J., Ed.; Wiley: Hoboken, NJ, USA, 1997; Volume 19, pp. 99–215.
28. Gimsing, A.L.; Kirkegaard, J.A. Glucosinolates and Biofumigation: Fate of Glucosinolates and Their Hydrolysis Products in Soil. *Phytochem. Rev.* **2009**, *8*, 299–310. [CrossRef]
29. Björkman, M.; Klingen, I.; Birch, A.N.E.; Bones, A.M.; Bruce, T.J.A.; Johansen, T.J.; Meadow, R.; Mølmann, J.; Seljåsen, R.; Smart, L.E.; et al. Phytochemicals of *Brassicaceae* in Plant Protection and Human Health—Influences of Climate, Environment and Agronomic Practice. *Phytochemistry* **2011**, *72*, 538–556. [CrossRef] [PubMed]
30. Bellostas, N.; Sørensen, J.C.; Sørensen, H. Profiling Glucosinolates in Vegetative and Reproductive Tissues of Four *Brassica* Species of the U-Triangle for Their Biofumigation Potential. *J. Sci. Food Agric.* **2007**, *87*, 1586–1594. [CrossRef]
31. Fourie, H.; Ahuja, P.; Lammers, J.; Daneel, M. *Brassicacea*-Based Management Strategies as an Alternative to Combat Nematode Pests: A Synopsis. *Crop Prot.* **2016**, *80*, 21–41. [CrossRef]
32. Brown, P.D.; Morra, M.J.; McCaffrey, J.P.; Auld, D.L.; Williams, L., III. Allelochemicals Produced during Glucosinolate Degradation in Soil. *J. Chem. Ecol.* **1991**, *17*, 2021–2034. [CrossRef] [PubMed]
33. Neubauer, C.; Heitmann, B.; Müller, C. Biofumigation Potential of *Brassicaceae* Cultivars to *Verticillium Dahliae*. *Eur. J. Plant Pathol.* **2014**, *140*, 341–352. [CrossRef]
34. Borek, V.; Elberson, L.R.; McCaffrey, J.P.; Morra, M.J. Toxicity of Isothiocyanates Produced by Glucosinolates in *Brassicaceae* Species to Black Vine Weevil Eggs. *J. Agric. Food Chem.* **1998**, *46*, 5318–5323. [CrossRef]
35. Jensen, J.; Styrishave, B.; Gimsing, A.L.; Hansen, H.C.B. The Toxic Effects of Benzyl Glucosinolate and Its Hydrolysis Product, the Biofumigant Benzyl Isothiocyanate, to *Folsomia Fimetaria*. *Environ. Toxicol. Chem.* **2010**, *29*, 359–364. [CrossRef]
36. Morra, M.J.; Kirkegaard, J.A. Isothiocyanate Release from Soil-Incorporated *Brassica* Tissues. *Soil Biol. Biochem.* **2002**, *34*, 1683–1690. [CrossRef]
37. Bellostas, N.; Sørensen, J.C.; Sørensen, H. Qualitative and Quantitative Evaluation of Glucosinolates in Cruciferous Plants during Their Life Cycles. *Agroindustria* **2004**, *3*, 5–10.
38. Kirkegaard, J.A.; Sarwar, M. Biofumigation Potential of *Brassicas* I. Variation in Glucosinolate Profiles of Diverse Field-Grown *Brassicas*. *Plant Soil* **1998**, *201*, 71–89. [CrossRef]
39. Kuai, J.; Sun, Y.; Zhou, M.; Zhang, P.; Zuo, Q.; Wu, J.; Zhou, G. The Effect of Nitrogen Application and Planting Density on the Radiation Use Efficiency and the Stem Lignin Metabolism in Rapeseed (*Brassica napus* L.). *Field Crops Res.* **2016**, *199*, 89–98. [CrossRef]
40. *ISO 9167-1*; Rapeseed—Determination of Glucosinolates Content—Part 1: Method Using High-Performance Liquid Chromatography. ISO: Geneva, Switzerland, 1992.
41. Yi, G.E.; Robin, A.H.K.; Yang, K.; Park, J.I.; Hwang, B.H.; Nou, I.S. Exogenous Methyl Jasmonate and Salicylic Acid Induce Subspecies-Specific Patterns of Glucosinolate Accumulation and Gene Expression in *Brassica oleracea* L. *Molecules* **2016**, *21*, 1617. [CrossRef] [PubMed]
42. Lake, L.; Sadras, V.O. Associations between Yield, Intercepted Radiation and Radiation Use Efficiency in Chickpea. In Proceedings of the 18th Australian Society of Agronomy Conference, Ballarat, Australia, 24–28 September 2017; Armstrong, R.D., Hafner, L., Eds.; Australian Society of Agronomy: Ballarat, Australia, 2017; pp. 24–28.

43. Wang, S.; Wang, E.; Wang, F.; Tang, L. Phenological Development and Grain Yield of Canola as Affected by Sowing Date and Climate Variation in the Yangtze River Basin of China. *Crop Pasture Sci.* **2012**, *63*, 478–488. [CrossRef]
44. Manevski, K.; Lærke, P.E.; Jiao, X.; Santhome, S.; Jørgensen, U. Biomass Productivity and Radiation Utilisation of Innovative Cropping Systems for Biorefinery. *Agric. Meteorol.* **2017**, *233*, 250–264. [CrossRef]
45. Larkin, R.P.; Griffin, T.S. Control of Soilborne Potato Diseases Using *Brassica* Green Manures. *Crop Prot.* **2007**, *26*, 1067–1077. [CrossRef]
46. Winde, I.; Wittstock, U. Insect Herbivore Counteradaptations to the Plant Glucosinolate-Myrosinase System. *Phytochemistry* **2011**, *72*, 1566–1575. [CrossRef]
47. Sarwar, M.; Kirkegaard, J.A. Biofumigation Potential of *Brassicas* II. Effect of Environment and Ontogeny on Glucosinolate Production and Implications for Screening. *Plant Soil* **1998**, *201*, 91–101. [CrossRef]
48. Torrijos, R.; Righetti, L.; Cirlini, M.; Calani, L.; Mañes, J.; Meca, G.; Dall'Asta, C. Phytochemical Profiling of Volatile and Bioactive Compounds in Yellow Mustard (*Sinapis alba*) and Oriental Mustard (*Brassica juncea*) Seed Flour and Bran. *LWT* **2023**, *173*, 114221. [CrossRef]
49. Ashiq, S.; Edwards, S.; Watson, A.; Blundell, E.; Back, M. Antifungal Effect of *Brassica* Tissues on the Mycotoxigenic Cereal Pathogen *Fusarium Graminearum*. *Antibiotics* **2022**, *11*, 1249. [CrossRef] [PubMed]
50. Ríos, P.; Obregón, S.; González, M.; de Haro, A.; Sánchez, M.E. Screening *Brassicaceous* Plants as Biofumigants for Management of *Phytophthora Cinnamomi* Oak Disease. *For. Pathol.* **2016**, *46*, 652–659. [CrossRef]